Direct Determination of Lead Speciation in Contaminated Soils by EXAFS Spectroscopy

ARTICLE *in* ENVIRONMENTAL SCIENCE AND TECHNOLOGY · APRIL 1996

Impact Factor: 5.33 · DOI: 10.1021/es9505154

Environ. Sci. Technol. **1996**, *30,* 1540−1552

Direct Determination of Lead Speciation in Contaminated Soils by EXAFS Spectroscopy

ALAIN MANCEAU,*,† MARIE-CLAIRE BOISSET,‡ GÉRALDINE SARRET,† JEAN-LOUIS HAZEMANN,† MICHEL MENCH,§ PHILIPPE CAMBIER,|| AND RENÉ PROST||

Environmental Geochemistry Group, LGIT-IRIGM, University of Grenoble and CNRS, BP53, 38041 Grenoble, Cedex 9, France, Laboratoire de Minéralogie−Cristallographie, Université Paris 6 et CNRS, 4 Place Jussieu, 75252 Paris, Cedex 05, France, INRA, Unité de Recherches Agronomie, Centre de Bordeaux, BP81, 33883 Villenave d'Ornon, Cedex, France, and Science du Sol, INRA, Route de St Cyr, 78026 Versailles, Cedex, France

Direct determination of the chemical form of trace metals in soils still remains a challenge for instrumental analytical techniques. This paper examines the potential of EXAFS spectroscopy to speciate and quantify the form of trace metals in the solid fraction of soil materials using lead as a case study. Three soils contaminated by different sorts of industrial activities, including the synthesis of lead organometallics for gasoline antiknocks, Pb−Zn smelting, and recycling of lead acid battery, were investigated. In soil contaminated by alkyl-tetravalent lead compounds, lead was found to be divalent and complexed to salicylate and catechol-type functional groups of humic substances. Lead sulfate and silica-bound lead are the predominant forms in the vicinity of the battery reclamation area. Near the smelter, lead was found to be divalent and coordinated to O,OH ligands. It is present in several chemical forms, which prevented them from being identified individually. The multiplicity of lead species in soils contaminated by smelting activities is thought to be due to long-term atmospheric emissions and to the variety of lead-containing phases simultaneously, and successively, emitted in the atmosphere. EXAFS can be applied to a wide variety of matrices including sediments, solid and liquid wastes, and fly ash particles.

* Corresponding author e-mail address: manceau@lgit.obsv-gr.fr; fax: 33-76-51-44-22.

† University of Grenoble and CNRS.

‡ Université Paris 6 et CNRS.

§ Unité de Recherches Agronomie.

|| Science du Sol.

Introduction

Soils, whether in urban or agricultural areas, represent a major sink for metals released into the environment from a variety of anthropogenic sources. Once in soil, some of these metals will be persistent because of their fairly immobile nature. Other metals, however, will be more mobile migrating to either groundwater aquifer or plants (bioavailability). There is a large consensus among the scientific community to believe that the risks for living organisms associated to the presence of heavy metals (HM) in our environment is determined for a large part by the solubility of the various HM-bearing phases present rather than by the total elemental concentration. As a consequence, knowledge of the total concentration of HM in soils provides only limited information, as this does not show how strongly the metal is bound to soil constituents. By identifying those HM-bearing phases and their solubility in aqueous fluids, one can infer the potential mobility and bioavailability of toxic metals. This information on the chemical forms of metals in a soil is therefore vital to assessing the hazard that these contaminations represent, and it can also guide the choice of remediation technologies.

Speciation of metals in soils has attracted much attention during the last decade. However, direct determination of the chemical form of trace metals is a difficult task. The relatively high dilution and the structural and chemical complexity of host matrices makes direct determination a challenge for instrumental analytical techniques. Indirect approaches were developed, which fractionate trace metals into forms of different solubilities and mobilities. Operationally defined sequential extraction procedures have been designed (*1*, *2*) and have been increasingly used over the last 10 years for determining the chemical form of metals in soils and sediments (see, e.g., refs 3−6). Recently, the European Commission has adopted a normalized sequential extraction protocol, which has been set up by a group of laboratories (*7*). The reproducibility of results was assessed by interlaboratory measurements, and this harmonized procedure is intended to become an international ISO or CEN standard. However, as pointed out by Quevauviller (*7*), in operationally defined procedures the "forms" of a metal are defined by the nature of the extractant, and it is certainly unwise to interpret the results in term of "metal speciation" because chemical extractants have no solid and chemical selectivity. In addition, even if the evaluation of "carbonate-bound" or "iron−manganese oxide-bound" forms had some real significance, this indirect approach does not provide information on the actual relationship, at a molecular level, between the metal and the phase in question. Indeed, metals may interact with solids in a variety of processes, including adsorption, absorption, surface precipitation, and coprecipitation, but they can also have precipitated in a pure oxide or salt form. These physicochemical processes determine the actual crystal chemical status of trace elements and, consequently, their fate and impact on the environment. Thus, to speciate and quantify the form of metals in structurally and chemically complex heterogeneous matrices such as soils, sediments, and various wastes, a selective and nondestructive technique is highly desirable.

0013-936X/96/0930-1540$12.00/0

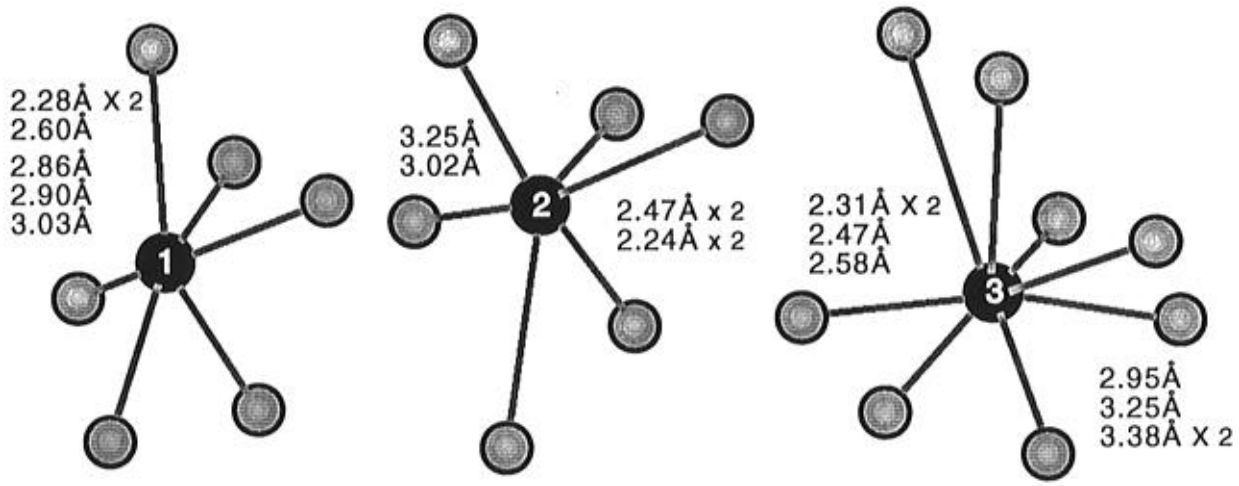

FIGURE 1. Three Pb coordination sites in $PbSiO_3$. Note the extremely high incoherence of Pb−O distances; after ref 24.

The development of the synchrotron radiation-based EXAFS technique during this last decade has enabled several groups to study directly the interaction of metals with isolated soil constituents (*8*, *9*). The knowledge gained during the past years on model compounds now makes it possible to apply this technique to real situations. Thus, it is the primary goal of this paper to report for the first time the potential and the limitations of EXAFS to speciate heavy metals in the solid fraction of contaminated soils. Speciation here refers to the determination of the different bonding forms and electronic structure (oxidation state, nature of chemical bonds) of an element. Four major bonding mechanisms can be distinguished for metal accumulation: (i) precipitation of discrete metal compounds (e.g., metal salt or oxide), (ii) complexation with organic matter, (iii) adsorptive bonding on fine grained particles (e.g., on oxides, silicates, ...), and (iv) incorporation in soil minerals through coprecipitation or lattice diffusion.

The biogeochemical cycle of lead has been affected by man to a greater extent than that of most other toxic metals (*10*). Through time, enormous amounts of anthropogenic lead have been stored in the biosphere, and its loading rate would exceed its natural removal rate (i.e., weathering mobilization) by about 20-fold or more (*11*). The use of lead by humans started before the Christian era, but its accumulation in the environment has risen rapidly since the Industrial Revolution as a result of human activities such as mining and smelting, acid battery recycling, synthesis of tetraalkyl lead and lead paints, and combustion of leaded gasoline (*12*). From about 1970, the United States and other countries limited the use of lead additives in petrol. Following these policy initiatives, lead concentrations in Greenland ice and snow have decreased by a factor of 7.5 (*13*). Lead is known for being fairly immobile in organic soils, with a transfer coefficient in the soil−plant system as low as 0.01−0.1 (*14*) and a mean residence time evaluated from hundreds to thousands of years (*15*−*17*). Accordingly, the reduction of environmental emissions will have little short-term effect on its accumulation in this compartment. Considerable evidence is available to explain its low mobility and bioavailability due to complexing by soil organic matter (*18*, *19*), but no direct evidence on natural samples has been provided to date, and the molecular mechanism of this retention remains unknown.

Background

Outline of EXAFS Spectroscopy. EXAFS spectra are obtained by measuring the X-ray absorption or fluorescence of a given sample as a function of the wavelength. The spectral scan is performed in the vicinity of an X-ray absorption edge of a chosen target element. It is therefore an element-specific, bulk-sensitive, and nondestructive method. Unlike most of spectroscopic methods, however, all heavy metals are spectroscopically active, and their spectral features do not overlap since their K or L edges are separated by several hundreds of electronvolts. This method can therefore be used to speciate successively heavy metals in compositionally complex matrices by sequentially tuning to one of their absorption edges. A detailed description of the physical principle of the method and of the data reduction is not attempted here; readers in search of this information are referred to recent textbooks on this subject (*20*). Geochemical and environmental applications have been recently reviewed (*8*, *9*, *21*).

Lead possesses specific electronic and structural properties that make it difficult to study by analytical techniques. In the following, we give a brief account of these specificities, particularly with respect to the spectral analysis and sensitivity of the EXAFS spectroscopy to the local structure of lead in various phases likely to be encountered in soils.

Coordination Chemistry of Lead. Lead can be tetravalent or divalent. The former oxidation state prevails in organic and the latter in inorganic lead chemistry. Divalent lead possesses a $6s^2$ outer shell electronic configuration. These two lone pair electrons are often stereochemically active and induce a strong deformation of divalent lead polyhedra (*22*). Another source of complexity comes from the high variability of its coordination number. Practically, all possible coordinations between 3 and 12 have been described in the literature (*23*). This complexity of the coordination chemistry of lead can be exemplified by lead silicate, $PbSiO_3$. In this solid, lead atoms occupy three different crystallographic sites. Pb(1) and Pb(2) sites can be considered 3- and 4-fold coordinated only if the nearest oxygens are taken into account or considered 6-fold coordinated if the next-nearest oxygens located at about 3 Å are considered to participate in the chemical bond with Pb atoms. The Pb(3) site is even less defined with four nearest oxygens at 2.31−2.58 Å and four others at 2.95−3.38 Å (Figure 1; *24*).

TABLE 1

Structural Coordination Environment of Lead in Reference Compounds[a]

compd	method	R_1	σ_1	N_1^X	R_2	σ_2	N_2^X	R_3	σ_3	N_3^X	coord. no.	ref
α-PbO	XRD	2.31	0	4^O							4	56
β-PbO	XRD	2.24	0	2^O	2.48		2^O				4	57
β-PbO_2	XRD	2.16	0	6^O							6	58
$PbSiO_3$	XRD	2.27	0.03	2^O	2.52	0.07	$\approx 1.6^O$	2.95	0.07	2^O	3,4	24
$PbSO_4$	XRD	2.67	0.06	6^O	2.96	0.05	4^O	3.27	0	2^O	12	59
$PbCO_3$	XRD	2.69	0.05	9^O	3.07	0.05	3^C	3.59	0.06	3^C	9	23
$Pb(NO_3)_2$	XRD	2.75	0	6^O	2.87	0	6^O	3.21	0	6^N	12	60
$PbCl_2$	XRD	2.87	0.01	3^{Cl}	3.07	0.01	4^{Cl}	3.63	0	2^{Cl}	9	61
$Pb(CH_3COO)_2$	XRD	2.47	0	1^O	2.62	0	4^O	2.86	0.08	3^O	8	62
$Pb(CH_3)_4$	Theory	2.24	0	4^C							4	63, 64

[a] R, interatomic distance. σ, standard deviation for interatomic distances. Coord. no., total coordination number. N^X, number and nature of atoms in the corresponding atomic shell.

The coordination chemistry of lead in a number of reference compounds is reported in Table 1. Due to the large incoherence of interatomic distances, atoms of the same nature, and for which distances from the central Pb atom differ by less than ≈0.15 Å, were grouped in the same atomic shell. Largest standard deviations are observed in $PbSiO_3$, $PbSO_4$, and $PbCO_3$. From the structural analysis of many lead compounds, we came to the conclusion that they can be classified into four groups on the basis of their Pb−nearest and −next-nearest atomic neighbor distances. In increasing distance order these are Pb^{4+}-containing solids (β-PbO_2, lead tetra(m)ethyl), lead monoxides (α/β-PbO), Pb^{2+} coordination compounds (lead acetate, citrate, salicylate), and lead salts (nitrate, sulfate, carbonate, chloride). The Pb−ligand distance in solids obviously depends on the oxidation state and the coordination number of lead. Largest distances are observed in salts. In salts, Pb^{2+} coordination numbers are so high that the limit of the lead coordination shell is difficult to determine precisely, making ill-defined the geometry of polyhedra.

Similar to the static disorder, the thermal vibration of Pb atoms in solids may also be high. The Debye temperature of elemental lead, which refers to the rigidity of Pb−Pb bonds, is as low as 105 K, thus accounting for the softness of lead metal. This temperature is unknown in our reference and soil compounds, but it may incidentally be low as well.

Consequences of static and dynamic structural disorders of lead compounds on EXAFS spectroscopy are several. First, EXAFS oscillations are smeared out, making it difficult to obtain a high signal to noise ratio spectrum above 10−12 $Å^{-1}$. This relatively limited reciprocal space range seriously decreases the distance resolution of the method and prevents the differentiation of elementary distances associated with the various atomic pairs. Second, when the disorder is anharmonic, the classical EXAFS analysis yields results that exclude the full distribution of interatomic distances (*20*). So, it may be unwise to give too much weight to coordination number calculations. Third, when the motion of atoms is high, their vibration is often also anharmonic, and interatomic distances determined from room temperature spectra are too short. These effects can be exemplified with $PbSiO_3$. Figure 2 compares its EXAFS spectra and radial distribution functions (RDFs) recorded at 295 and 10 K. The dramatic loss of intensity at room temperature is noteworthy. Note also the short distance shift of the first RDF peak at room temperature, which attests for the existence of strong anharmonic effects. A quantitative analysis of these spectra resulted in 1.5 O at 2.27 Å (σ = 0.08 Å) + 0.6 O at 2.46 Å (σ = 0.10 Å) at 295 K and 1.5 O at 2.29 Å (σ = 0.06 Å) + 0.7 O at 2.69 Å (σ = 0.07 Å) at 10 K. This example shows that EXAFS spectroscopy does not resolve individual interatomic crystallographic distances and yields a weighted average of the various structural environments of lead atoms in $PbSiO_3$. In addition, the total number of oxygen neighbors recovered by this analysis is notably lower than that expected from X-ray diffraction even at low temperature, a consequence of the anharmonic static disorder.

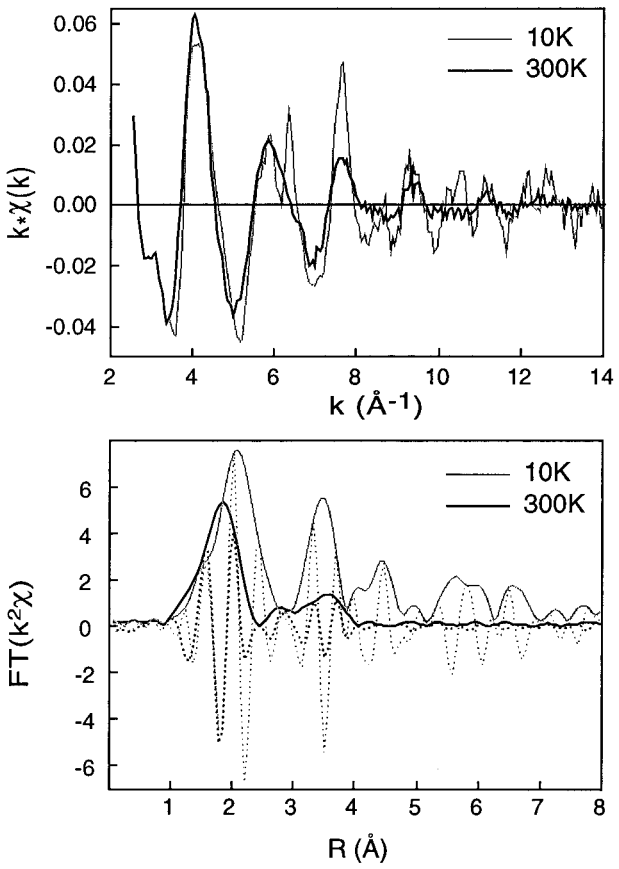

FIGURE 2. Pb L_{III}-EXAFS and Fourier transform for $PbSiO_3$ at 300 and 10 K. The envelope curves, also called radial distribution functions, are the magnitude of the complex Fourier transform ± $(Re^2 + Im^2)^{1/2}$, and the oscillary curves are the imaginary part of the transform.

For the reasons invoked previously, extreme care is needed for recording high quality and for quantitatively interpreting lead EXAFS spectra. These intrinsic difficulties faced by experimentalists partly explain the scarcity of EXAFS studies performed to this point on this widespread element. It will be shown below that EXAFS spectra

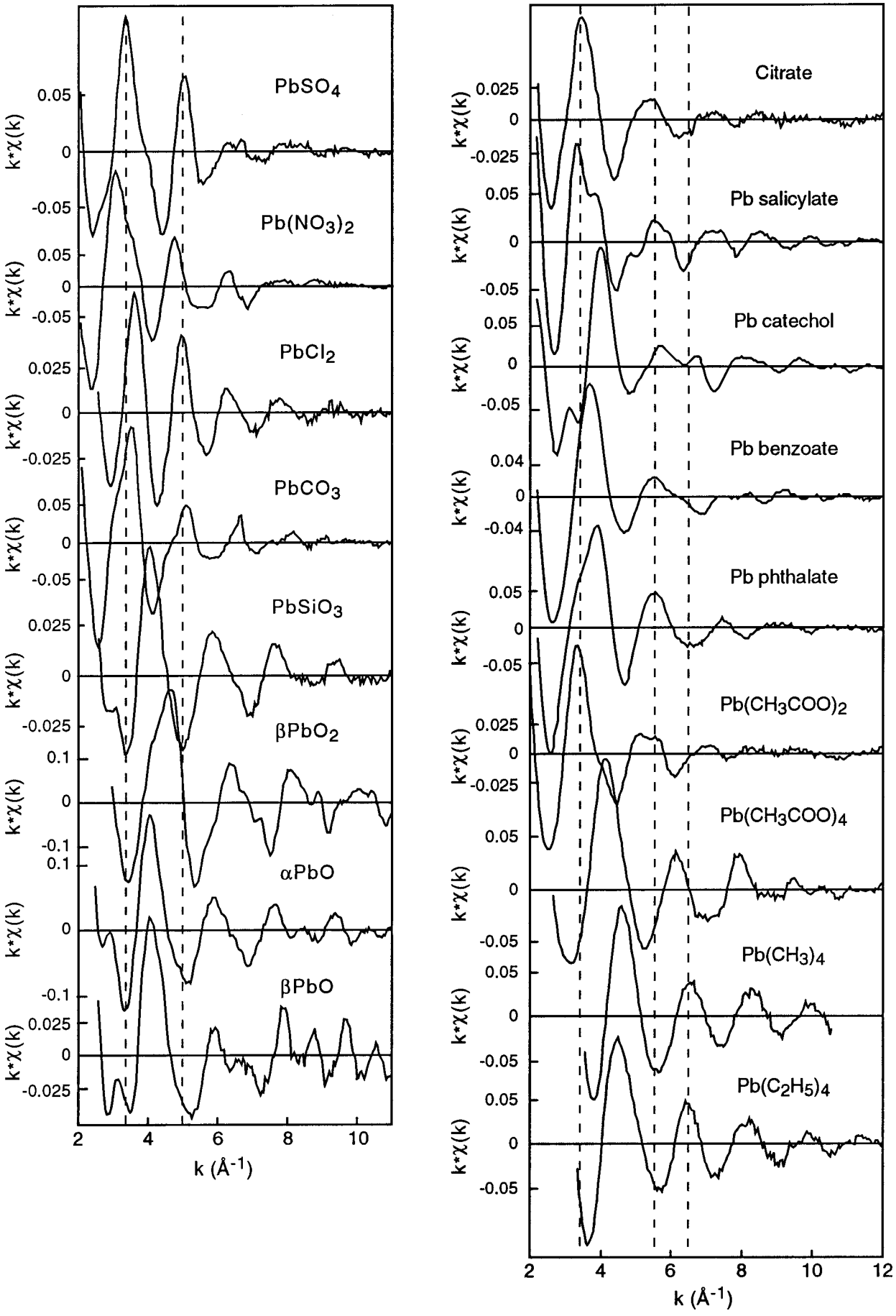

FIGURE 3. Pb L_{III}-EXAFS spectra for lead reference compounds.

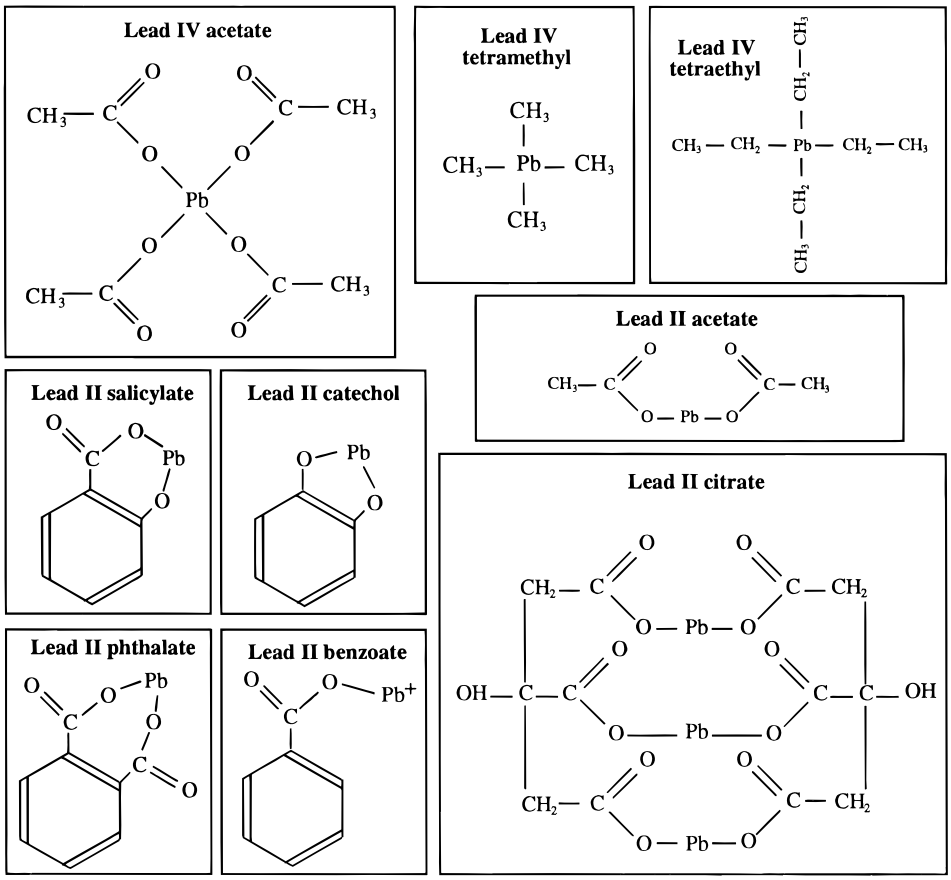

FIGURE 4. Developed chemical formula of some lead coordination and organolead compounds.

however exhibit a shape that reflects the nearest-neighbor coordination geometry of lead and thus can be used as a powerful structural fingerprint of its coordination environment in matrices as complex as soils.

Sensitivity of EXAFS Spectroscopy to Lead Speciation. Figure 3 contrasts Pb L_{III}-EXAFS spectra for a large variety of lead inorganic and organic compounds. Pb L_{III}-EXAFS probes the structural environment around Pb up to a distance of 3−4 Å. Therefore, any change in the nearest atomic neighbor environment of lead should normally be detected in the EXAFS spectra. Figure 3 shows the ease with which precipitated lead species can be identified by this method. Specifically, α/β-PbO (Pb^{2+}) and β-PbO_2 (Pb^{4+}) on one hand and $Pb(CH_3COO)_2$ (Pb^{2+}) and $Pb(CH_3COO)_4$ (Pb^{4+}) on the other, exemplify the valence-specific spectral shape of EXAFS spectra. Dependence of spectral shape on the nature of second and third nearest atomic neighbors can be appraised by comparing spectra for coordination and alkyllead compounds (Figures 3 and 4). Specifically, lead tetraethyl and tetramethyl spectra bear subtle but clearly distinctive differences pertaining to the presence of four CH_3 next-nearest groups in the former alkyllead compound. Likewise, the binding of lead to phenolic OH and carboxylic COOH groups as in salicylate yields an EXAFS spectrum readily distinguishable from the others. From the structural analysis of reference spectra, it was concluded in the previous section that lead compounds could be classified in four groups on the basis of their average Pb−nearest neighbors distances. Figure 5a contrasts spectra for lead salicylate, sulfate, oxide, and tetraethyl, which are representative of these groups. Examination of this figure shows that an unknown sample can readily be classified in one of these groups by simply looking at the phase of its electronic wave.

This fingerprinting approach is not restricted to the identification of precipitated forms of lead but applies also to forms that are fixed to soil constituents. Recent works conducted on model systems have greatly extended our knowledge of the sorption and lattice substitution mechanisms of trace metals in a large variety of soil minerals, including iron, manganese, and aluminum oxides (*25*−*33*), clays (*34*), carbonates (*35*, *36*), and phosphates (*37*). We now possess a reasonably good understanding of mechanisms whereby trace metals interact with soil minerals to enable us to recognize such processes directly from the analysis of soil EXAFS spectra. As an example of the sensitivity of the method to different soil fixation processes, Figure 5b compares the L_{III}-EXAFS spectra for lead sorbed on hydrous ferric oxide and the manganese dioxide, birnessite. Examination of this figure shows that the two Pb−EXAFS spectra are markedly distinct.

In conclusion, the comparison of reference EXAFS spectra for lead precipitates and soil-sorbed forms showed that this technique can be used to fingerprint the structural environment of lead in multielement and multiphasic matrices. It will be applied in the following to identify and compare lead species in soils contaminated by different sorts of industrial activities.

Materials and Methods

Samples Description. Three French soils contaminated by lead fallout were selected to compare lead speciation in sites impacted by different industrial activities including the synthesis of lead organometallics for gasoline antiknock

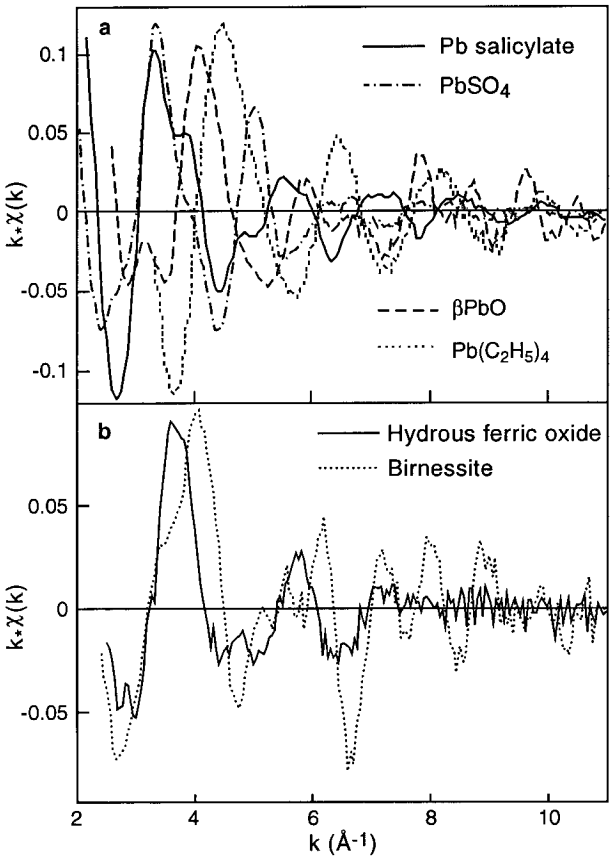

FIGURE 5. (a) Comparison of Pb L_{III}-EXAFS spectra for lead salicylate, sulfate, oxide, and tetraethyl. (b) Pb L_{III}-EXAFS spectra for lead sorbed hydrous ferric oxide, after ref 28, and lead sorbed birnessite (unpublished results).

compounds, recycling of lead acid batteries, and Pb−Zn smelting. The first site (P) was located in an old garden situated in the proximity of an alkyllead production plant (*38*). The soil sample was collected in the top 4-cm layer. After sonification and sedimentation in pure water, the <2-μm fraction was selected for this study. It contained 1.67 g/kg total Pb and 17 g/kg total C. Powder X-ray diffraction indicated the presence of smectite, mica, kaolinite, quartz, and feldspar. The second site (B) was located in the area of a former lead battery reclamation facility, which closed operation several years ago. Sample B1 was collected in a grassland located 100 m from the factory (pH = 7.1). Sample B2 was collected on the former factory site (pH = 5.7). The two B soils are sandy and contain, besides prevalent quartz, mica and kaolinite. These two samples were analyzed as collected, and their lead content amounted to 3200 (B1) and 52 000 mg/kg (B2). Sample E comes from the surface layer (0−25 cm) of a cultivated soil located 1 km from a Pb−Zn smelter. The 0.2−2-μm fraction was studied and contained 4500 mg/kg lead. Its clay fraction consists essentially of montmorillonite. Trace of kaolinite, mica, quartz, and lepidocrocite were detected by powder X-ray diffraction.

Method. X-ray absorption spectra were collected at ambient temperature on the wiggler magnet beamline 9.2 at the DRAL Synchrotron Radiation Source (SRS) at Daresbury, Warrington (U.K.). The electron storage ring operated at 2 GeV with an average beam current of ~200 mA. A Si(220) double-crystal monochromator was used. Higher harmonic reflections were rejected by detuning the primary beam by 30−50%. Gas ionization chambers were filled with argon/helium mixture to attenuate the beam intensity by 20% before and 80% after the samples for transmission mode measurements. Pb-rich samples and references were measured in transmission mode. Spectra for less concentrated samples were collected in fluorescence mode using a 13-element Ge array detector with a Be window. Multiple scans (3−8 depending on Pb concentration) were collected and averaged for each sample to improve the signal-to-noise ratio.

Data Reduction. X-ray absorption spectra were treated following a standard procedure (*20*). Pb L_{III}-edge EXAFS spectra were derived from raw absorption spectra by normalization to the atomic absorption jump. The zero ionization energy of the 2p electron (E_0) was chosen at the midpoint of the absorption edge for all spectra. Note that the absolute position of absorption maxima in EXAFS spectra depends on the choice of E_0, but this factor is not critical since the modeling approach developped in the present study relies on relative peak displacements between unknown and reference spectra. The kinetic energy of the photoelectron was converted into the modulus of the wavevector **k** to obtain the $\chi(k)$ function. This function is the summation of the elementary contributions to the EXAFS spectra of the very first atomic shells surrounding lead. The atomic pair correlation function, or radial distribution function (RDF), was obtained by Fourier transforming $k^2*\chi(k)$ spectra to real space using a Kaiser apodization window (*39*). RDFs are not corrected for atomic pair phase shift functions, and thus each peak is displaced toward short distances by approximatively $\Delta R \approx 0.3-0.4$ Å from its crystallographic position. Extraction of structural parameters, namely, interatomic distance (R) and coordination number (CN), characterizing the atomic environment of Pb atoms was accomplished by Fourier back-transforming in momentum space (k) one or several RDF peaks(s). This yields the contribution to the EXAFS spectrum of the atomic shell(s) attached to the selected RDF peak(s), and this experimental Fourier-filtered partial contribution to the EXAFS spectrum was then least-square fitted by a theoretical curve. These simulations require the knowledge of phase-shift and amplitude functions for each atomic pair under consideration. These functions were determined empirically from model compounds.

Results and Discussion

EXAFS spectra for the four soil samples are plotted in Figure 6. These spectra are markedly different since none of the oscillations are in phase. Drastic differences are observed specifically for B1 and B2 despite their close sampling sites. This comparison immediately indicates that the speciation of lead in these different soil materials is not the same. Differences in the atomic environment of lead from one sample to another are clearly apparent on RDFs (Figure 7). Their structural differences comprise peak position, number, intensity, and phase of the imaginary part. RDFs for samples P and E exhibit very weak second and third atomic shell contributions beyond the first and intense low distance Pb−ligand peak at 2 Å. This weakness of the amplitude is due to either the presence of low-Z nearest atomic neighbors (i.e., C, O, ...) as their X-ray back-scattering amplitude is low or to the existence of a range of different structural environments about lead atoms as in $PbSiO_3$. It will be demonstrated below that the former hypothesis stands for the sample P and the latter for E. The shape of the RDF for B2 stands in strong contrast to the three others as it

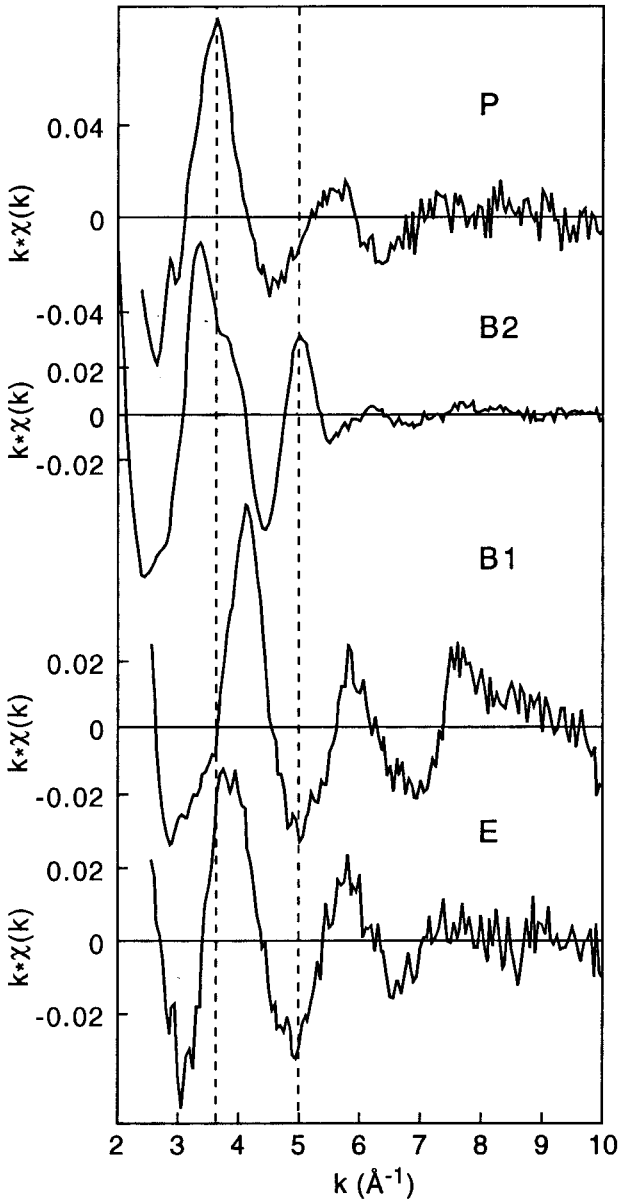

FIGURE 6. L_{III}-EXAFS spectra from soil samples

exhibits a broad and strong second peak, attesting the existence of ordered second and third metal shell contributions. This observation allows us to exclude the presence in this sample of organically bound lead.

The low intensity or broadness of second and third RDF peaks make their quantitative analysis particularly difficult. It proved highly preferable to work directly on raw EXAFS spectra rather than on Fourier-filtered contributions as it is usually done in EXAFS data reduction (*20*). In the following, we shall compare individually these soil EXAFS spectra to those of a selection of model compounds.

Alkyllead Contamination. Tetraalkyllead species, which are at the origin of this pollution, were released into the environment by evaporation. Volatile R_4Pb species exist primarily in the vapor phase in the atmosphere and have half-lives of a few hours. When exposed to air, they are progressively broken down by hydroxyl radicals to a variety of trialkyl and dialkyl species, of which the trialkyl species predominate with estimated half-lives of 5 days (*40*, *41*). Monoalkyllead exists only as a transient intermediate in the breakdown to inorganic lead, the final product of alkyllead emissions. The disappearance of alkyllead species

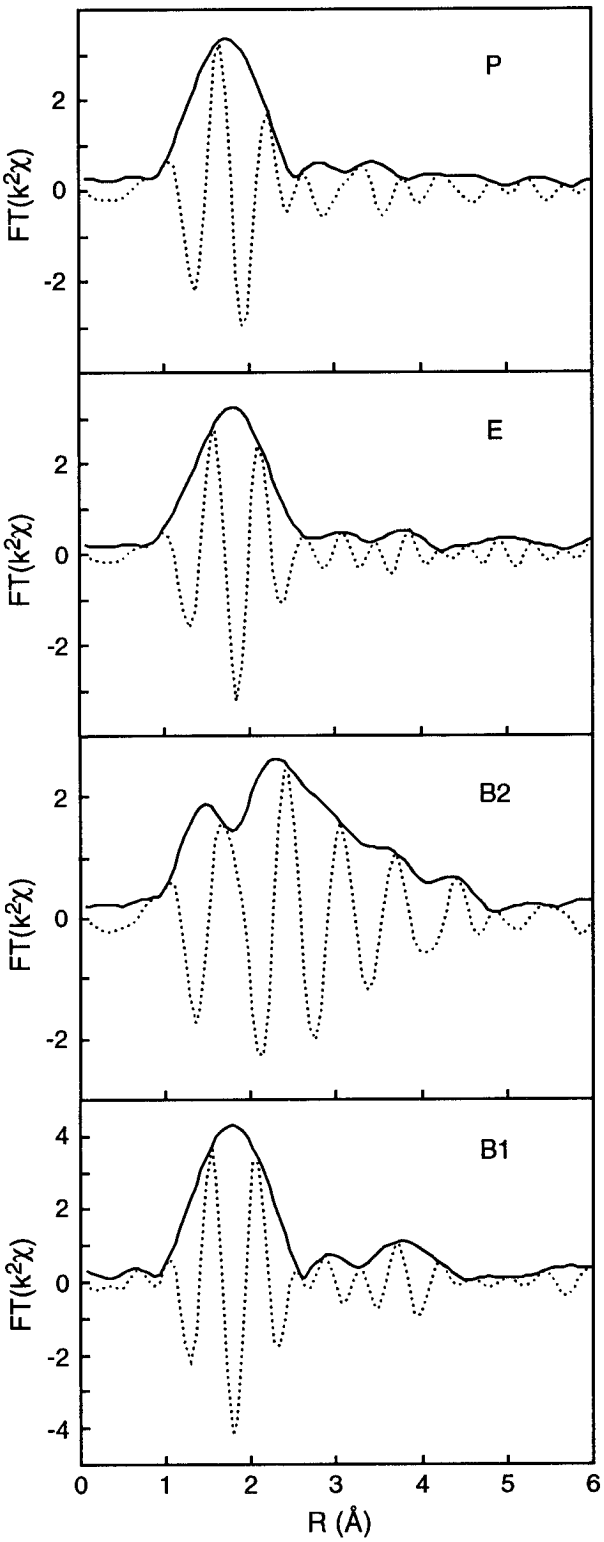

FIGURE 7. RDFs for soil samples.

is attested by Figure 8 where P and lead tetraethyl spectra are overplotted. On the basis of spectral comparisons, the presence of lead salt (nitrate, sulfate, chloride, phosphate), oxide precipitate, and aliphatic lead carboxylate complex can also be ruled out. Obtaining a reasonable spectral match could only be achieved by assuming a complexing of divalent lead to carboxylate or OH groups attached to an aromatic ring (Figure 4). However, it is clear from Figure 8 that, based on EXAFS spectra frequencies and amplitude, the chemical form of lead in sample P differs substantially

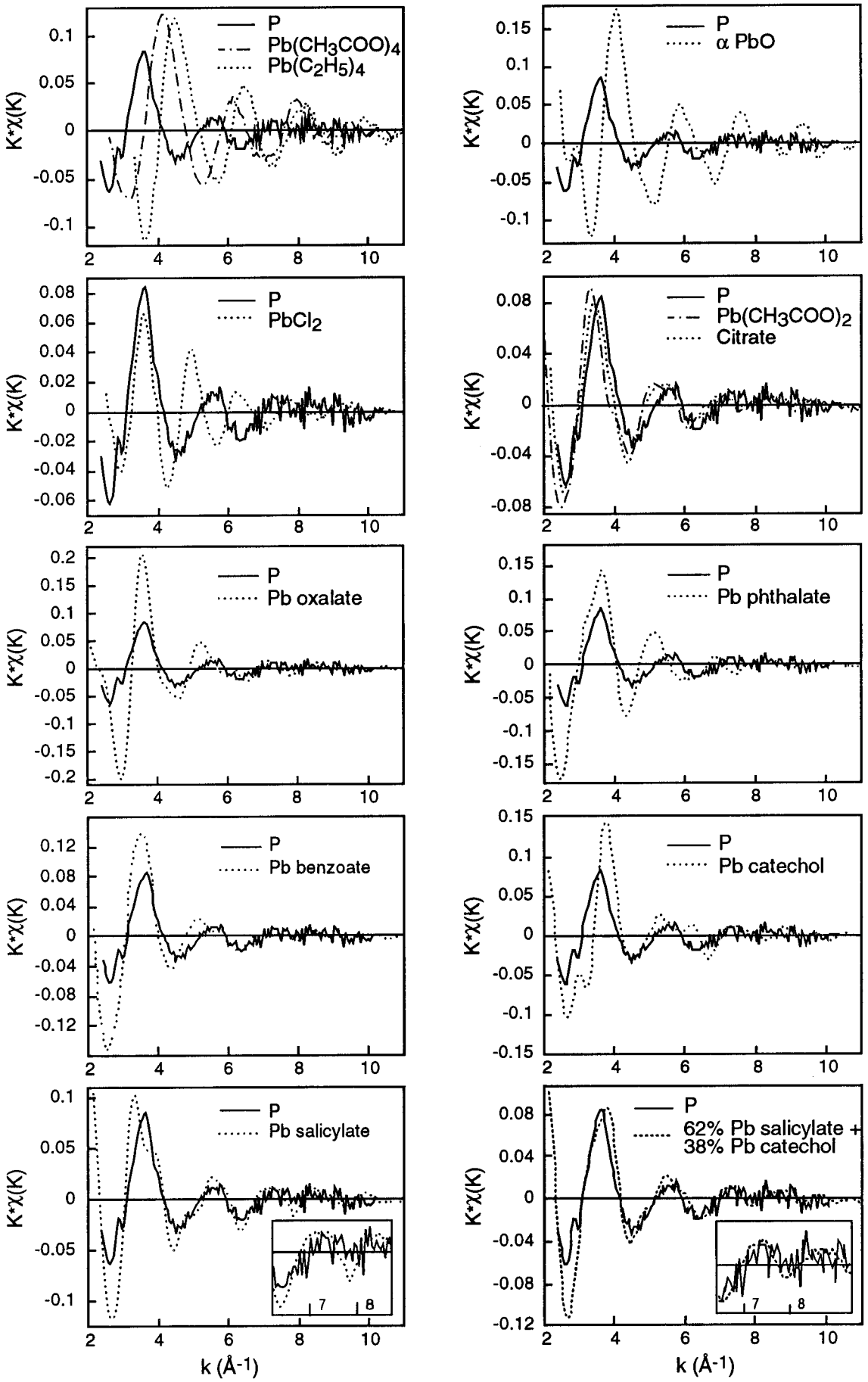

FIGURE 8. Comparison of the EXAFS spectrum for the alkyllead-contaminated soil with those of a selection of lead crystalline reference compounds.

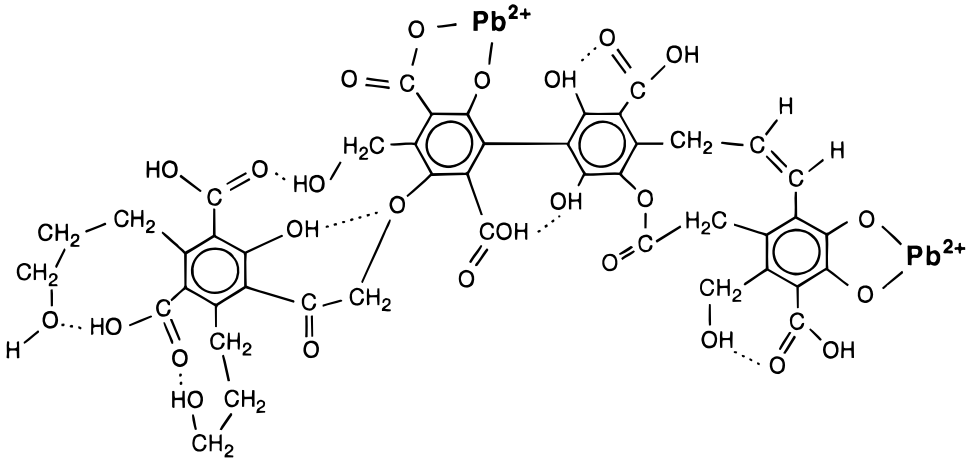

FIGURE 9. Complexation mechanism of lead by humic substance. The model structure of the humic substance is from ref 55.

from phthalate and benzoate. The salicylate reference was found to be the nearest fit for this natural sample, and the features in the two spectra are very similar. The major differences encompass the slight downshift of the salicylate first oscillation crest, which peaks at 3.5 $Å^{-1}$, and the small misfit of its third wave oscillation centered at 7 $Å^{-1}$ (see inset). This observation suggests the presence of other substitutional forms. This possibility was investigated by digitally combining EXAFS spectra of the different coordination compounds available to us. The best spectral resemblance was obtained by assuming a mixture of salicylate (60%) and catechol (40%) functional groups. Figure 8 shows that the soil and combined spectrum look very close to each other over the entire 3−9 $Å^{-1}$ range. It should be emphasized that this procedure is different from the normal spectral fitting generally employed to quantitatively interpret EXAFS spectra. There, several parameters are varied to construct a theoretical spectrum that best fits the experimental one. Here, linear combinations of the experimentally obtained spectra are made to construct an unknown mixture. However, for the reasons evoked in the section on the coordination chemistry of lead, Pb−EXAFS spectra are relatively featureless, and reference spectra are not significantly different from each other. Consequently, the precision on the determination of the relative proportion of lead complexes is relatively low, and it was found that varying the proportion of salicylate and catechol forms within 10−20% had minor effects on the general shape of the combined spectrum. Therefore, it is estimated that there is an upper limit of 20% error in the method.

The spectral similarity of this soil sample with model organic compounds unambiguously indicates that lead is complexed by organic matter, and a schematic structural representation of a lead humic substance is given in Figure 9. This finding is in agreement with laboratory experiments conducted on model systems. The ability of humic and fulvic acids to form stable complexes with metal ions has been known for a long time and has been attributed to their high content of O-containing functional groups, including carboxylic COOH; phenolic, alcoholic and enolic OH; and ketonic C═O structures of various types (*42*−*44*). Carboxylate groups are by far the most abundant. For instance, the acidity of COOH groups in fulvic acids was evaluated to range from 520 to 1120 cmol (H^+) kg^{-1} for a total acidity between 640 and 1420 cmol (H^+) kg^{-1} (*43*). But despite the high concentration of COOH groups, it was showed that metal ions are predominantly complexed to humic substances by phenolic OH and carboxylic COOH groups located in ortho position, i.e., by salicylate-type functional groups (*45*−*47*). Chelation of metals by COOH (benzoate-type complex), two adjacent COOH (phthalate-type complex), or OH (catechol-type) groups are also possible but seem to be of a lesser quantitative importance as compared to salicylate (*48*−*51*). The present study provides the first compelling structural evidence for the complexing of lead by salicylate-type and catechol-type functional groups in natural and undisturbed soil humic substances. The strength of these two Pb^{2+}−humic acid bidentate complexes provides a molecular level explanation for the high residence time of lead in organic soils.

Battery Recycling Contamination. *Sample B1.* The EXAFS spectrum of sample B1 has been plotted in Figure 10 along with a selection of references. The fingerprinting analysis indicates that lead is divalent and belongs to the soil mineral fraction. As is noted in Figure 10c,d, the spectral pattern and oscillation crests of lead monoxides, lead silicate ($PbSiO_3$), and B1 are very similar. However, lead monoxides and B1 spectra differ by their amplitude, which indicates that if α/β-PbO were really present in this soil, they would coexist with other lead species. However given the close resemblance of B1 and $PbSiO_3$ spectra, lead seems in all likelihood to be predominantly associated with silica. This finding is corroborated by the comparison of RDFs (Figure 11a,b). The intensity of Pb−O and Pb−Pb peaks in α-PbO is twice as high as that of Pb−nearest neighbor peaks in sample B1. Examination of Figure 11a shows also that the imaginary part of the second and third RDF peaks are not precisely in phase. Overplotting RDFs for B1 and $PbSiO_3$ yields close amplitude and phase match (Figure 11b).

Minor differences between B1 and $PbSiO_3$ EXAFS spectra and RDFs can be accounted for by the presence of ancillary lead species. Their nature was inferred by performing linear combinations of reference spectra. Figure 12a shows that a very good spectral match could be obtained by assuming 85% $PbSiO_3$ + 3% $PbSO_4$. A second computationally correct solution was obtained by assuming 46% β-PbO + 10% α-PbO + 2% $PbSO_4$. In our opinion, this latter solution should be rejected because it implies that there exist other unknown lead constituents present that amount to ≈40% of total lead. In addition, this interpretation would mean that the spectral similarity between B1 and $PbSiO_3$ is purely circumstantial. The presence of a silica-bound lead phase appears very likely because this soil is sandy and lead may have precipitated with free silicic acid or at the surface of

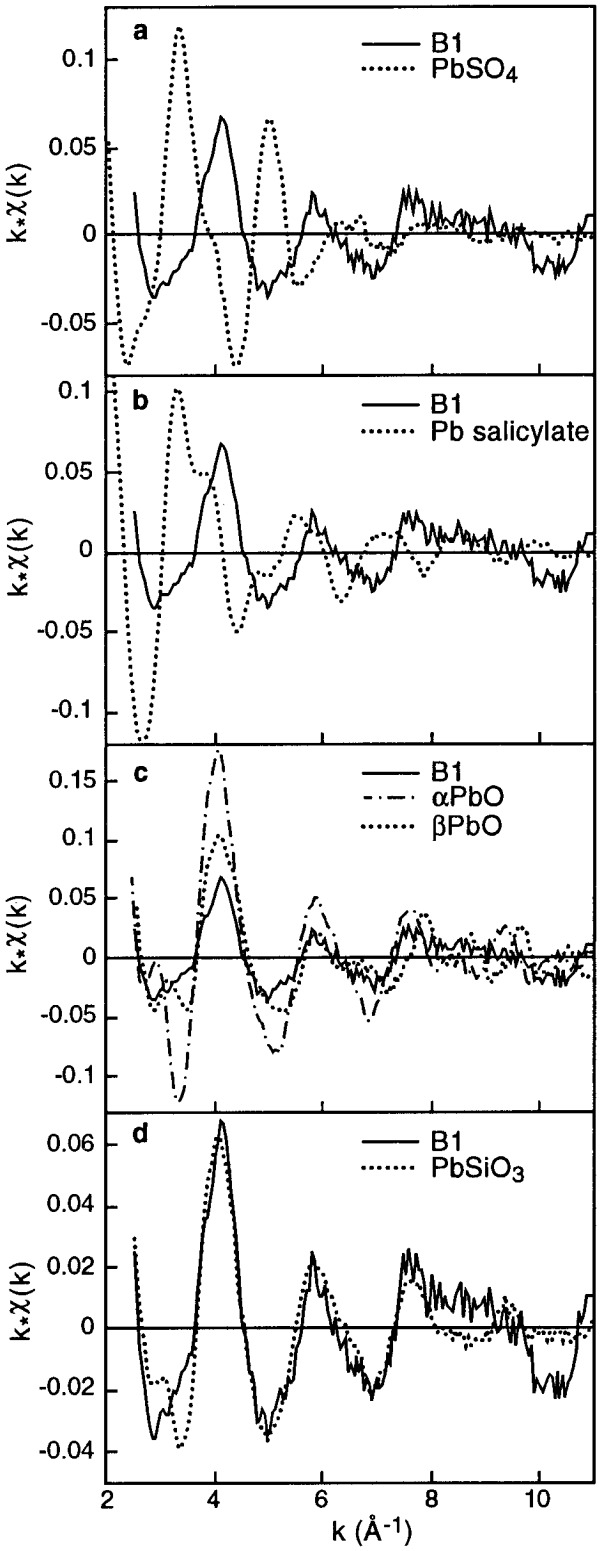

FIGURE 10. Comparison of the EXAFS spectrum for sample B1 with those of a selection of lead crystalline reference compounds.

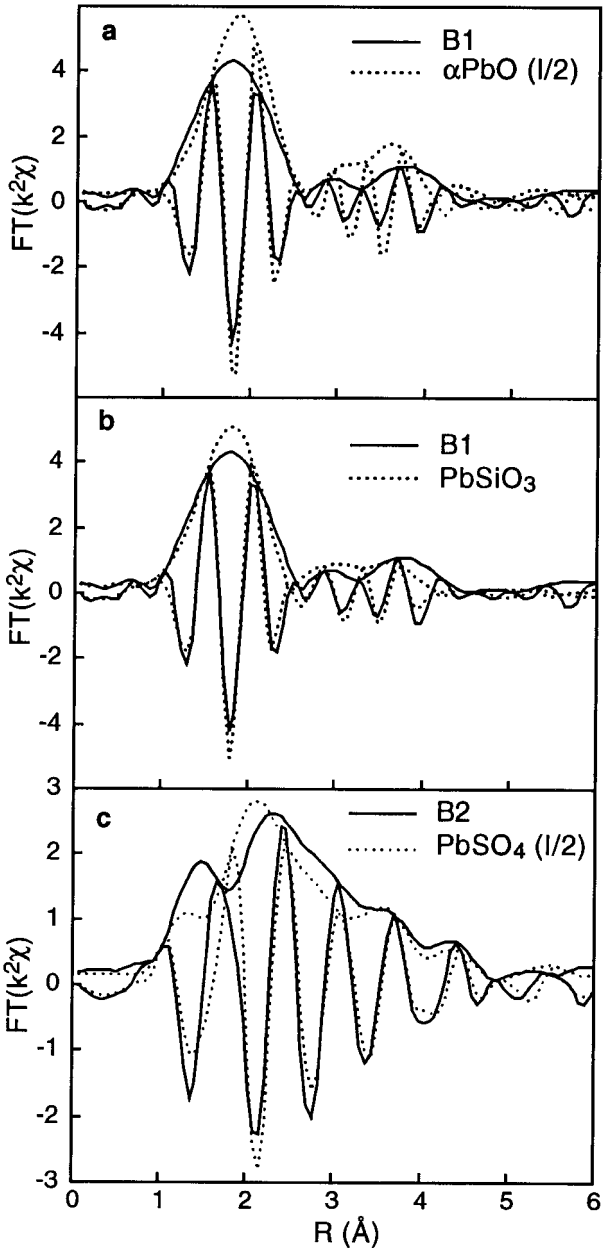

FIGURE 11. Comparison of RDFs for B1 and α-PbO (a), B1 and $PbSiO_3$ (b), and B2 and $PbSO_4$ (c).

quartz grains consecutively to its adsorption. This interpretation is strengthened by solution chemistry studies, which showed that the solubility product of lead silicates is low and that surface complexation constants for lead sorbed on silica and quartz are high (*52*). The contribution of $PbSO_4$ is negligible, and less than 5% of the lead is believed to be present as sulfate.

Sample B2. The spectral analysis of sample B2 indicates that lead is predominantly present as a divalent salt. The closest resemblance was obtained with $PbSO_4$ and $PbCl_2$ (Figure 13). The presence of lead chloride should be rejected due to the low activity of chloride ions in this soil and the origin of the pollution since lead batteries contain lead sulfate as a result of the corrosion of lead electrodes by sulfuric acid used as electrolyte (*53*). The close match in shape and phase of RDFs for B2 and $PbSO_4$ is really striking, but their difference in amplitude suggests that the lead-bearing phase is not unique (Figure 11c). Similarly to sample B1, two spectral combinations produced as good fit: 57% $PbSO_4$ + 13% β-PbO + 6% α-PbO and 59% $PbSO_4$ + 39% $PbSiO_3$ (Figure 12b). Even though the sensitivity of the technique is not high enough for differentiating these two solutions, this analysis allows us to ascertain the presence of lead sulfate in this soil. However, the ambiguity between lead oxide and silica-bound lead could not be clarified.

Old batteries contain elemental lead, lead oxide, lead sulfate, and sulfuric acid (*54*). The presence of large amount

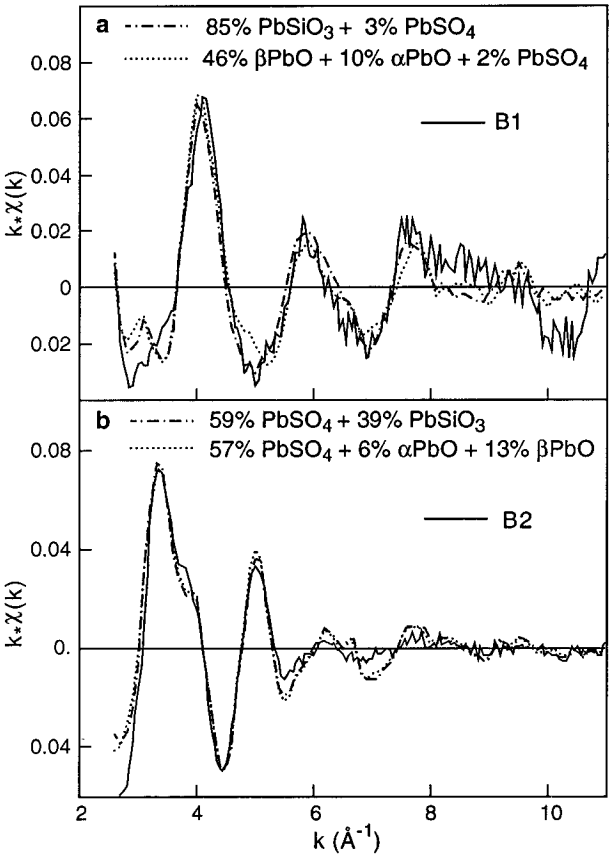

FIGURE 12. L_{III}-EXAFS spectrum of sample B1 (a) and B2 (b) compared with constructed spectra. Spectral adjustments were performed by least square fitting various combinations of reference spectra.

of $PbSO_4$, and presumably of some trace amount of lead oxide, likely originates from the on-site storage of waste material. However, the precipitation of lead silicate cannot be dismissed. Old battery cases are usually stored as a pile on the ground prior to Pb recovery, spilled sulfuric acid can then facilitate the movement of divalent lead ions contained in the battery fluid through the soil. Free lead ions may have reacted with silica and precipitated as in the site B1. Based on this scenario, sites B1 and B2 would differ solely by the degree of incorporation of lead to soil materials. At the location of the former storage site, the rejection of lead sulfate was probably so high that after several years of industrial inactivity lead is only partly incorporated in soil constituents, being predominantly present as lead sulfate. In the vicinity of the reclamation facility the concentration of lead sulfate is lower and Pb retention is now likely controlled by coprecipitation with soil silica or precipitation at the surface of quartz grains. The nature of atmospheric emission is not known by us, but the presumed formation of a silica-bound lead phase suggests that lead was ejected in the atmosphere as an easily degradable form.

Pb−Zn Smelting Contamination. The analysis of this sample led us to reject the presence of organically bound lead and lead salt (Figure 14). The EXAFS spectrum for this sample bears some resemblance with lead monoxides and silicate, but no good fit could be obtained with any of the reference compounds available to us. The amplitude of this spectrum is extremely low, being even lower than that of lead silicate $PbSiO_3$, the amplitude of which is already particularly low compared to other lead-containing compounds due to its high structural disorder. By comparison with $PbSiO_3$, the very low intensity of spectrum E attests

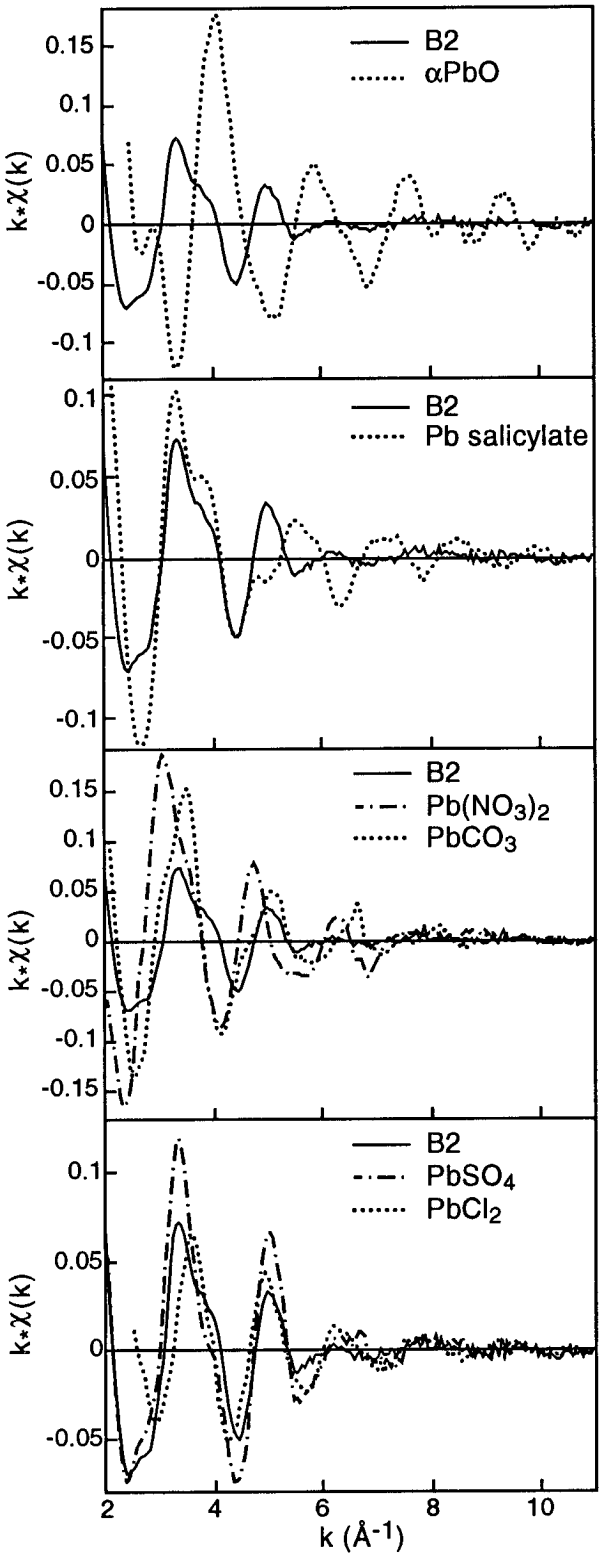

FIGURE 13. Comparison of the EXAFS spectrum for the sample B2 with those of a selection of lead crystalline reference compounds.

to the existence of a wide range of Pb−(O,OH) and Pb−nearest cation interatomic distances. The most likely explanation for this phenomenon is the presence in this soil of multiple divalent lead species.

The multiplicity of lead forms can be understood by considering the nature of atmospheric emissions by the smelter. Lead−zinc sulfurs were originally treated by a pyrometallurgic process, which has been subsequently replaced by a hydrometallurgic process. Accordingly, the

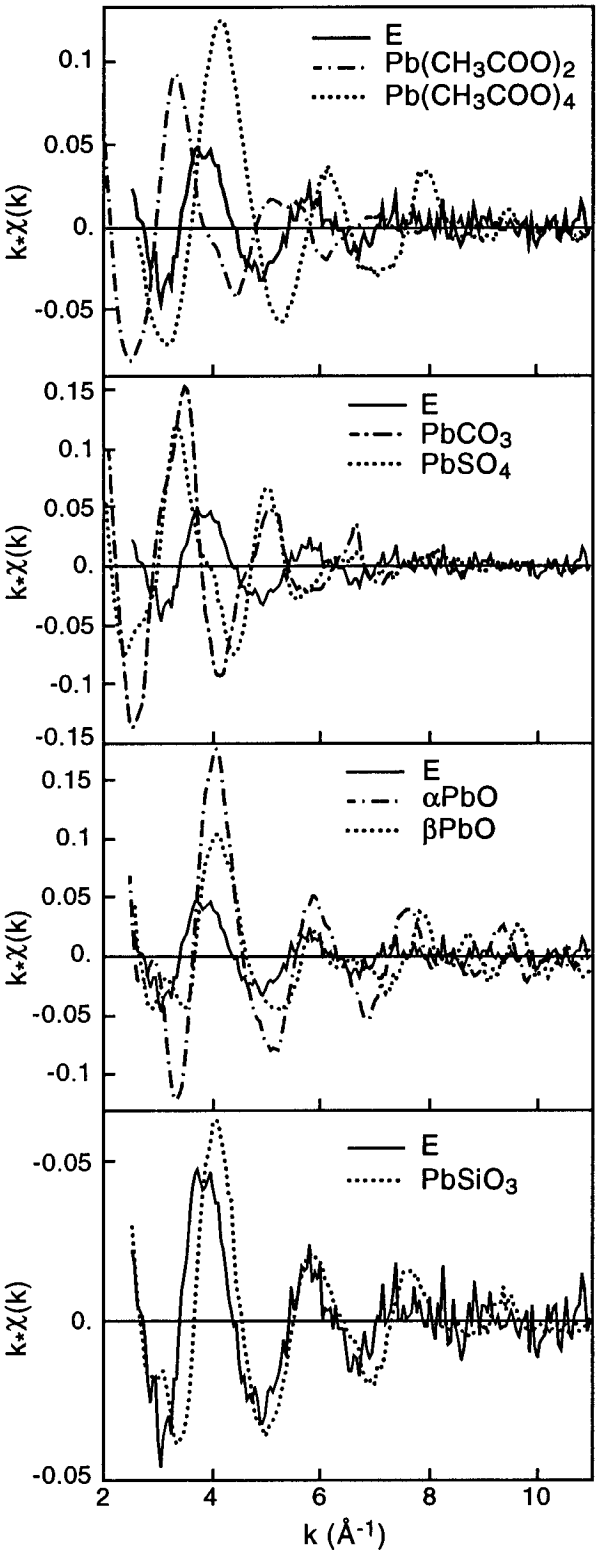

FIGURE 14. Comparison of the EXAFS spectrum for the sample E with those of a selection of lead crystalline reference compounds.

nature of products released in the atmosphere has changed along time. In addition, for a given period of time, lead is thought to have been emitted in different forms such as oxides and sulfates. Facing the high temporal and instantaneous variability in the nature of lead product emissions, it may not be surprising to find that lead is present in surrounding soils in a number of different chemical forms. Identifying their nature remains a challenge, which is certainly beyond the capacity of any existing analytical method.

Acknowledgments

The authors are grateful to the staff at the Synchrotron Radiation Source in Daresbury Laboratory for their technical support and wish to acknowledge the use of the Chemical Database Service. This work was supported by the French Ministry of Environment, Grants 925 675 and 91125.

Literature Cited

(1) Tessier, A.; Campbell, P. G. C.; Bisson, L. *Anal. Chem.* **1979**, *51*, 844−851.
(2) Salomons, W.; Förstner, U. *Environ. Tech. Lett.* **1980**, *1*, 506−518.
(3) Sheppard, M. I.; Thibault, D. H. *Soil Sci. Soc. Am. J.* **1992**, *56*, 415−423.
(4) Belazi, A. U.; Davidson, C. M.; Keating, G. E.; Littlejohn, D. *J. Anal. At. Spectrom.* **1995**, *10*, 233−240.
(5) Davidson, C. M.; Thomas, R. P.; Mcvey, S. E.; Perala, R.; Littlejohn, D.; Ure, A. M. *Anal. Chim. Acta* **1994**, *291*, 277−286.
(6) Whalley, C.; Grant, A. *Anal. Chim. Acta* **1994**, *291*, 287−295.
(7) Quevauviller, P.; Rauret, G.; Muntau, H.; Ure, A. M.; Rubio, R.; Lopezsanchez, J. F.; Fiedler, H. D.; Griepink, B. *Fresenius J. Anal. Chem.* **1994**, *349*, 808−814.
(8) Brown, G. E. In *Mineral-Water Interface Geochemistry*; Hochella, M. F., White, A. F., Eds.; Mineralogical Society of America: Washington, DC, 1990; pp 309−364.
(9) Charlet, L.; Manceau, A. In *Environmental Particles*; Buffle, J., Van Leeuwen, H. P., Eds.; Lewis Publishers: Chelsea, MI, 1993; pp 117−164.
(10) Alloway, B., Ed. *Heavy metals in soils*; Blackie Academic & Professional: Glasgow, 1995.
(11) Nriagu, J. O. In *Heavy metals in the environment*; Farmer, J. G., Ed.; CEP Consultant ltd.: Edinburgh, 1991.
(12) Hong, S.; Candelone, J. P.; Patterson, C. C.; Boutron, C. F. *Science* **1994**, *265*, 1841−1843.
(13) Boutron, C. F.; Görlasch, U.; Candelone, J. P.; Bolshov, M. A.; Delmas, R. J. *Nature* **1991**, *353*, 153−156.
(14) Kloke, A.; Sauerbeck, D. R.; Vetter, H. In *Changing Metal Cycles and Human Health*; Nriagu, J. O., Ed.; Springer-Verlag: Berlin, 1984; pp 113−141.
(15) Benninger, L. K.; Lewis, D. M.; Turekian, K. K. In *Marine chemistry in the coastal environment*; Church, T. M., Ed.; American Chemical Society Symposium Series 18; American Chemical Society: Washington, DC, 1975; pp 201−210.
(16) Heinrichs, H.; Mayer, R. *J. Environ. Qual.* **1977**, *6*, 402−407.
(17) Heinrichs, H.; Mayer, R. *J. Environ. Qual.* **1980**, *9*, 111.
(18) Stevenson, F. J. *Soil Biol. Biochem.* **1979**, *11*, 493−499.
(19) Bizri, Y.; Cromer, M.; Scharff, J. P.; Guillet, B.; Roullier, J. *Geochim. Cosmochim. Acta* **1984**, *48*, 227−234.
(20) Teo, B. K. *EXAFS: Basic Principles and Data Analysis*; Inorganic Chemistry Concepts 9; Springer-Verlag: Berlin, 1986.
(21) Manceau, A.; Harge, J. C.; Sarret, G.; Hazemann, J. L.; Boisset, M. C.; Mench, M.; Cambier, P.; Prost, R. Prost, R., Eds. Submitted.
(22) Galy, J.; Meunier, G.; Andersson, S.; Astrom, A. *J. Solid State Chem.* **1975**, *13*, 142.
(23) Sahl, K. *Z. Kristallogr.* **1974**, *139*, 215−222.
(24) Boucher, M. L.; Peacor, D. R. *Z. Kristallogr.* **1968**, *126*, 98−111.
(25) Charlet, L.; Manceau, A. *J. Colloid Interface Sci.* **1992**, *148*, 25−442.
(26) Manceau, A.; Llorca, S.; Calas, G. *Geochim. Cosmochim. Acta* **1987**, 105−113.
(27) Manceau, A.; Rask, J.; Buseck, P. R.; Nahon, D. *Am. Mineral.* **1990**, *75*, 490−494.
(28) Manceau, A.; Charlet, L.; Boisset, M. C.; Didier, B.; Spadini, L. *Appl. Clay Sci.* **1992**, *7*, 201−223.
(29) Manceau, A.; Charlet, L. *J. Colloid Interface Sci.* **1994**, *168*, 87−93.
(30) Manceau, A. *Geochim. Cosmochim. Acta* **1995**, *59*, 3647−3653.
(31) Spadini, L.; Manceau, A.; Schindler, P. W.; Charlet, L. *J. Colloid Interface Sci.* **1994**, *168*, 73−86.
(32) Chisholm-Brause, C. J.; Hayes, K. F.; Roe, A. L.; Brown, G. E. J.; Parks, G. A.; Leckie, J. O. *Geochim. Cosmochim. Acta* **1990**, *54*, 1897−1909.
(33) Waite, T. D.; Davis, J. A.; Payne, T. E.; Waychunas, G. A.; Xu, N. *Geochim. Cosmochim. Acta* **1994**, *58*, 5465−5478.
(34) O'day, P. A.; Parks, G. A.; Brown, G. E. *Clays Clay Miner.* **1994**, *42*, 337−355.

(35) Pingitore, N. E. J. R.; Lytle, F. W.; Davies, B. M.; Eastman, M. P.; Eller, P. G.; Larson, E. M. **1992**, *56*, 1531−1538.
(36) Reeder, R. J.; Lamble, G. M.; Lee, J. F.; Staudt, W. J. *Geochim. Cosmochim. Acta* **1994**, *58*, 5639−5646.
(37) Sery, A.; Manceau, A.; Greaves, N. *Am. Mineral.* In press.
(38) Mench, M.; Amans, V.; Arrouays, D.; Didier-Sappin, V.; Fargues, S.; Gomez, A.; Löffler, M.; Masson, P. *Adv. Environ. Sci.* In press.
(39) Manceau, A.; Combes, J. M. *Phys. Chem. Miner.* **1988**, *15*, 283−295.
(40) Radojevic, M.; Harrison, R. M. *Atmos. Environ.* **1987**, 2403−2411.
(41) Harrison, R. M.; Turnbull, A. B.; Wang, Y. *Appl. Organomet. Chem.* **1993**, *7*, 567−572.
(42) Senesi, N. In *Biogeochemistry of Trace Metals*; Adriano, D. C., Ed.; Lewis Publishers: Chelsea, MI, 1992; pp 429−496.
(43) Stevenson, F. J. *Humus chemistry: Genesis, composition, reactions*; Wiley Interscience: New York, 1994.
(44) Senesi, N.; Miano, T. M. *Humic substances in the global environment and implications on human health*; Elsevier: New York, 1994; 1367 pp.
(45) Schnitzer, M.; Skinner, S. I. M. *Soil Sci.* **1965**, *99*, 278−284.
(46) Schnitzer, M. *Soil Sci. Soc. Am. Proc.* **1969**, *33*, 75−81.
(47) Gamble, D.; Schnitzer, M.; Hoffman, I. *Can. J. Chem.* **1970**, *48*, 3197−3204.
(48) Boyd, S. A.; Sommers, L. E.; Nelson, D. W. *Soil Sci. Soc. Am. J.* **1981**, *45*, 1241−1242.
(49) Piccolo, A.; Stevenson, F. J. *Geoderma* **1982**, *27*, 195−208.
(50) Prasad, B.; Dkhar, G. D.; Singh, A. P. *J. Indian Soc. Soil Sci.* **1987**, *35*, 194−197.
(51) Templeton, G. D.; Chasteen, N. D. *Geochim. Cosmochim. Acta* **1980**, *44*, 741−752.
(52) Schindler, P. W.; Fürst, B.; Dick, R.; Wolf, P. U. *J. Colloid Interface Sci.* **1976**, *55*, 469−475.
(53) Bullock, K. R.; Trischan, G. M.; Burrow, R. G. *J. Electrochem. Soc.* **1983**, *130*, 1283.
(54) Bullock, K. R. *J. Power Sources* **1994**, *51*, 1−17.
(55) Morel, F. M. M. *Principles of Aquatic Chemistry*; Wiley-Interscience: New York, 1983.
(56) Leciejewicz, J. *Acta Crystallogr.* **1961**, *14*, 1304.
(57) Hill, R. J. *Acta Crystallogr.* **1985**, *C41*, 1281−1284.
(58) D'Antonio, P.; Santoro, A. *Acta Crystallogr.* **1980**, *B36*, 2394−2397.
(59) Miyake, M.; Minato, I.; Morikawa, H.; Iwai, S. I. *Am. Mineral.* **1978**, *63*, 506−510.
(60) Nowotny, H.; Heger, G. *Acta Crystallogr.* **1986**, *C42*, 133−135.
(61) Nozik, Y. Z.; Fykin, L. E.; Muradyan, L. A. *Sov. Phys. Cristallogr.* **1976**, *21*, 38−40.
(62) Rajaram, R. K.; Rao, M. J. K. *Z. Kristallogr.* **1982**, *160*, 225−233.
(63) Kaupp, M.; Scleyer, P. R. *J. Am. Chem. Soc.* **1993**, *115*, 1061−1073.
(64) Oyamada, T.; Iijima, T.; Kimura, M. *Bull. Chem. Soc. Jpn.* **1971**, *44*, 2638−2641.

Received for review July 12, 1995. Revised manuscript received November 25, 1995. Accepted December 17, 1995.[⊗]

ES9505154

[⊗] Abstract published in *Advance ACS Abstracts,* March 1, 1996.